

INVESTIGATING THE IMPLEMENTATION OF USAF DAMAGE
TOLERANT RISK ANALYSIS WITH A STRUCTURAL
HEALTH MONITORING SYSTEM

by

JEFFREY SCOTT TIPPEY

Presented to the Faculty of the Graduate School of
The University of Texas at Arlington in Partial Fulfillment
of the Requirements
for the Degree of

MASTER OF SCIENCE ELECTRICAL ENGINEERING

THE UNIVERSITY OF TEXAS AT ARLINGTON

MAY 2011

Copyright © by Jeffrey Scott Tippey 2011

All Rights Reserved

ACKNOWLEDGEMENTS

My whole life I have been blessed to have a great friends and family in my life. I am the first to admit that I would have never gotten to this point without them. I would like to thank my beautiful wife, Amanda, for always being there for me. Amanda, I could not have done this without you and I want to thank you for being so patient and understanding with me, even when I was unable to give you the time you deserved. Also, I would like to thank my parents, Darold and Karen. Words cannot express how much you guys have done for me and I am so lucky to have you as my parents. I would like to thank my in-laws Bobby, Vicki, Robert, and Crese for letting me slide sometimes when schoolwork got in the way. In addition, I would like to thank Dr. Edward Kolesar. Ed, I am so thankful for the time I was able to work with you. You welcomed me in even though I was young and inexperienced and I am grateful for that. You were patient with me and I learned so much working with you. I consider myself lucky to have been able to work with you and I will miss you. In addition, I would like to thank Dale Ball. It was a pleasure getting to work with you, I learned so much. I really enjoyed our talks and I hope to continue them into the future. Dr. Kondraske, thank you for working with me and helping me to get started with the writing. It is funny how quick it goes after that. Dr. Liang, I appreciate your time and insights. I would like to thank Charlie, Kraig, and John for taking the time to help me out along the way. Finally, I would like to thank all my friends that I was unable to mention by name. I am so lucky to have you all.

April 15, 2011

ABSTRACT

INVESTIGATING THE IMPLEMENTATION OF USAF DAMAGE TOLERANT RISK ANALYSIS WITH A STRUCTURAL HEALTH MONITORING SYSTEM

Jeffrey Scott Tippey, M.S.

The University of Texas at Arlington, 2011

Supervising Professor: George V. Kondraske

The recent improvements in micro fabrication, power management, and distributed sensor networks have made Structural Health Monitoring (SHM) an appealing solution for decreasing costs, decreasing risk of catastrophic failure, and improving overall aircraft health and maintenance (Mukkamala, 2000). A SHM system uses non-destructive inspection (NDI) to provide on-demand updates on the health of a structure, such that the integrity of the structure can be quantified and accounted for (Achenback, 2009). In order to provide an accurate representation of a structure's health, a distributed network of sensors must work in unison to detect a distribution of cracks and damage present on the structure. Each individual sensor or groups of sensors maps a small portion of the structure and the information is then pooled together and processed to provide a representation of the structure's health at any specific instant in time.

This representation of the structure's health can then be used to perform a risk analysis which takes into account parameters such as; material properties, mission-loading assumptions, current damage, and time between inspections. These parameters are used to calculate an associated Probability of Fracture (POF) of an aircraft during flight, which can then be used to quantify the health of a

fleet of aircraft. Currently, the Air Force uses periodic visual inspections, magnetic-optical imaging (MOI) inspections, and risk analysis to quantify the readiness of its fleet. The goal of this thesis was to investigate the combination of the USAF Structural Risk Methodology with a SHM system and perform a risk analysis for a cargo aircraft. During the study, two different SHM sensor systems were combined with the USAF Structural Risk Methodology and the resulting risk of a cargo lift aircraft was calculated for both systems (P. Hovey A. B., 1998). It is our belief that a SHM system combined with the USAF Structural Risk Methodology can provide substantial savings in the management of the aircraft fleet by eliminating the need for frequent, time consuming, and expensive inspections.

TABLE OF CONTENTS

ACKNOWLEDGEMENTS	iii
ABSTRACT	iv
LIST OF ILLUSTRATIONS	viii
LIST OF TABLES	x
Chapter	Page
1. INTRODUCTION.....	1
1.1 Structural Health Monitoring	1
1.2 Defining POD and POF.....	3
1.2.1 Definition of POD	3
1.2.2 Definition of POF	4
1.3 The Challenge.....	4
1.4 Specific Objectives.....	5
2. SHM SYSTEMS	7
2.1 Elastic Wave Based SHM Systems	7
2.2 POD of Smart-Layer SHM System	9
2.2.1 Piezoelectric SHM System Experiment	11
2.3 Eddy Current SHM Systems	22
2.4 POD of Eddy-Current SHM System.....	23
3. USAF STRUCTURAL RISK METHODOLOGY	26
3.1 Structural Risk Analysis	26
3.2 USAF Structural Risk Model	28
3.3 USAF Inspection and Repair Model.....	32
4. EVALUATION STUDY OF USAF STRUCTURAL RISK METHODOLOGY BASED STRUCTURAL HEALTH MONITORING SYSTEM	3

5. CONCLUSION	39
REFERENCES.....	43
BIOGRAPHICAL INFORMATION	46

LIST OF ILLUSTRATIONS

Figure	Page
1. POD of Each Sensor Mapped To X,Y Coordinate	4
2. Most common types of damage for (a) metallic sheets (b) composite materials	6
3. (a) Current Air Force risk analysis process (b) Proposed risk analysis process with changes highlighted in yellow	7
4. (a) Passive piezoelectric SHM system (b) Active piezoelectric SHM system.....	9
5. Passive SHM System.....	9
6. Active SHM System	10
7. Illustration of cargo plane showing where sample was taken from	11
8. Test Subject was 4 frame wide by 7 frame panel	12
9. Piezoelectric SHM setup.....	13
10. Signal/sensor paths of piezoelectric SHM system	14
11. 5-peak modulated sine wave used to excite piezoelectric actuator.....	14
12. Typical piezoelectric sensor response	14
13. Location and orientation of twelve cracks added to the airframe	15
14. Diagnostics image of the no-damage baseline configuration	16
15. Direct Path image for crack 1.....	17
16. RBA image for crack 1	18
17. Initial Direct Path image for crack 2	19
18. Direct Path image of crack 2 with increased sensitivity	19
19. RBA analysis image of the crack 2	19
20. Direct Path image of crack 2 and crack 3	20
21. Direct Path image of cracks 2-6.....	20
22. Plot of calculated POD for piezoelectric SHM system	23

23. (a) 2 channel MWM array (b) 7 channel MWM Array	24
24. Estimated POD for eddy current SHM system.	25
25. Initial flaw size distribution.....	35
26. Crack growth as a function of service time.	35
27. PDF and CDF of fracture toughness.....	36
28. Probability of stress exceedance per flight	36
29. Piezoelectric SHM normalized single-flight probability of failure	37
30. Normalized SFPOF for eddy-current SHM system.....	38

LIST OF TABLES

Table	Page
1. Approximate limits of NDI crack detection techniques.....	3
2. Experimental results for piezoelectric SHM POD test	21
3. POF terms for case $a \leq ac$	31
4. POF terms for case $a > ac$	31

CHAPTER 1

INTRODUCTION

1.1 Structural Health Monitoring

Structural Health Monitoring (SHM) is a promising solution with potential to decrease lifecycle cost, decrease operational risks, and improve fleet health and readiness (Mukkamala, 2000). By creating an accurate model of a structure's health at specific instants in time, the resources used by traditional time and usage based maintenance schedules can be drastically reduced. In 1978, the National Bureau of Standards and Battelle Laboratories completed an exhaustive study that estimated the total cost associated with material fracture and failure in the United States to be over \$88 billion dollars per year; corresponding to almost 4% of the national GDP at the time (Shantz, 2010; R.P. Reed). The study concluded that substantial savings on materials, transportation, and capital investment costs were possible if technology transfer, combined with research and development, succeeded in reducing the variables of uncertainty relating to a structure's reliability over its lifetime (Shantz, 2010). Emphasis on fracture mechanics, material properties, and improved inspection schedules/techniques were discussed as potential methods of improving structural reliability, while reducing material usage and early replacement of healthy critical components (Shantz, 2010). Among the major industry sectors where fatigue and fracture of structural components are of critical concern and present a large opportunity for savings, is that of the aeronautical and aerospace industry (Shantz, 2010).

Originally, the aerospace industry used a safe life design approach to increase the structural integrity throughout the life of a structural component (Shantz, 2010). The safe life design method assumes components are flaw free and are designed and tested to withstand a pre-determined design life (Shantz, 2010). The average fatigue life of the structure is estimated and then divided by a subjective factor of safety in order to ensure safe operation over the operational lifetime of the component (Shantz, 2010). As soon as a component has reached its design lifetime, it is retired from service, regardless of its

current condition (Shantz, 2010). Since many components tend to be over designed, components are commonly retired long before their actual useful lives have been reached (Shantz, 2010). In addition, this analysis does not take into account defects that could cause failure before the intended design life has been reached, thus a damage tolerance approach was later adopted to overcome these limitations (Shantz, 2010).

The United States Air Force (USAF) became the first organization to formally require damage tolerance design with the issuance of MIL-A-83444 Airplane Damage Tolerance Requirements in 1974 (Shantz, 2010). MIL-A-83444 specifies that aircraft frames must be designed using the assumption that cracks are present at all critical locations within the structure (Shantz, 2010; A.F. Grandt, 2004). In damage tolerance design, every structure is initially assumed to have cracks present on the structure (Shantz, 2010). These cracks affect the strength of the structure and continue to propagate under cyclic loading conditions that are significantly lower than critical yield strength of the material and will ultimately lead to failure of the structure (Shantz, 2010). Damage tolerance analysis is based on fracture mechanics and has required engineers to develop a much better understanding of service loads and stress spectrums, material properties, and crack growth mechanisms (Shantz, 2010).

SHM uses non-destructive inspection (NDI) techniques to create an on-demand representation of the structure's health, which can then be used to perform operational risk analyses, such as Probability of Fracture (POF), and determine aircraft maintenance needs (Achenback, 2009). Some of the NDI techniques that have been used include ultrasonic scanning, liquid penetrant, magnetic particle, and eddy current probes (E. Larson, 2000). The USAF damage tolerant design handbook lists the approximate resolution of crack sizes that can be detected with the various NDI techniques (Shantz, 2010). They are listed in table 1. Of those methods listed in table 1, eddy current techniques and ultrasonic techniques are most commonly used for SHM applications.

Table 1. Approximate limits of NDI crack detection techniques (Shantz, 2010; J.P. Gallagher, 1984)

NDI Method	Minimum Detectable Crack (inches)
Liquid Penetrant	.09
Ultrasonic	0.07
Eddy Current	0.23
Magnetic Particle	0.07
Visual Inspection	0.25

As SHM technology has progressed, SHM systems have become more integrated allowing them to more accurately track the health of larger structures over periods of time, instead of a much more limited role of determining whether or not damage is present in small areas (Mukkamala, 2000). However, this integration comes with a steep price paid for in complexity in the system design and subsequent analysis software. Current SHM systems have not been utilized to their full cost saving potential because of a lack of quantification of SHM reliability. Thus, any further analysis should consider the upfront costs and sustainment costs for both SHM systems and manual inspection schedules. SHM systems have been known to rely on highly customized designs, which have limited their implementation to date. However when comparing both methods, one should also consider that manual inspections are unreliable, since they rely on human factors that do not lend themselves to easy quantification and thus require frequent inspections to keep acceptable levels of risk (A. Coppe, 2008). Currently, the Air Force uses frequent visual inspections and periodic magnetic-optical imaging (MOI) inspections and risk analysis to quantify the readiness of its fleet. For a cargo aircraft, the inspected areas can be very large making visual inspections time consuming and MOI inspections even more time consuming. It would be beneficial from a resource and cost perspective to reduce or eliminate the need for these inspections.

1.2 Defining POD and POF

1.2.1 Defining POD

Several assumptions that affect probability of detection (POD) are made to determine the POD for an integrated SHM monitoring system; however our goal is to develop a single POD function that can be used to quantify the POD for a crack of size, a , at any location in the structure. This subsequent POD will be used to analyze the proposed SHM risk analysis and plays a large part. To start, the probability of cracks and damage during operation is dependent on the area to be monitored and flight envelope of the aircraft. However, when calculating POD in this paper we assumed that a crack was equally likely to be at any location in the structure and equally likely to be orientated in any direction relative to the sensors. Another assumption that was made in this paper is that the POD for each sensor or set of sensors is a finite number between 0 and 1 that will map to a corresponding x and y location on the airframe, as shown in figure 1.

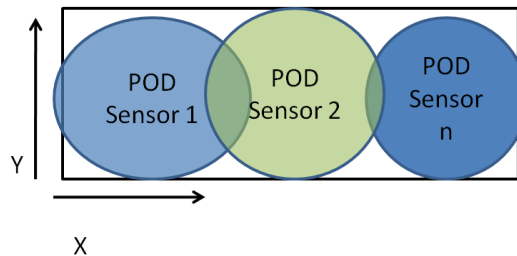


Figure 1. POD of Each Sensor Mapped To X,Y Coordinate

A POD for each sensor, 1 to n = the total number of sensors, will exist for every location on the structure, although it may effectively be 0 as the distance of the flaw from the sensor is increased. As a result, a single POD value was calculated for each SHM system by using a hit/miss analysis (Department of Defense, 2009). We attempted to maintain conservative viewpoint when determining POD because the experimental data set was not large enough to provide a definite POD curve. However, future studies with more data points should be performed before a similar system should be implemented in an aircraft.

Large data sets would provide the flexibility to use statistical models of the sensors to include sensor variance, statistical models of the structures properties, and the ability to use different types of sensors if desired by including a variance calculation that would give the probable ranges of POD for the system and a subsequent range of POD values (R. Guratzsch, 2010). This thesis used the methods discussed in MIL-HDBK-1823A “Nondestructive Evaluation System Reliability Assessment” to calculate a POD for the SHM system (Department of Defense, 2009). This POD was then used to develop a probabilistic risk based analysis that determined the single flight probability of failure (SFPOF).

1.2.2 Definition of POF

Probability of fracture (POF) is a measure of risk present on an aircraft structure during operation. In this thesis, POF was defined as the probability of a critical structural component failing during flight. We defined this as a catastrophic event where the structure is unable to support the load it is intended to support and designed the POF to remain below an acceptable risk level. The USAF Structural Risk Methodology uses probabilistic models of aircraft loading, material properties, and inspection/repair process to calculate the single-flight probability of failure (SFPOF) for an aircraft relative to maintenance inspection intervals.

1.3 The Challenge

In order to show a robust solution that can work regardless of the SHM sensor system used, a POD was estimated for an elastic-wave based SHM system and an eddy current based SHM system, both installed on similar structural configurations. One challenge identified during this thesis was the inherent difficulty associated with determining the POD of an elastic-wave based SHM system on metallic sheets. As metallic sheets are subjected to normal loads over extended periods of time they are prone to damage from cracks, as illustrated in figure 2 (a). Due to the linear geometry of a crack on a metallic sheet, the POD for an elastic wave SHM system is difficult to calculate in an elastic wave based SHM system. The interaction of the elastic wave with the crack is dependent on the length of the crack, the orientation, and the distance to the crack (V. Giurgiutiu, 2005). In addition, the interaction is also highly

dependent on the wavelength of the elastic wave, the material, and the geometry of the structure, making it difficult to accurately predict. Whereas in a composite material, the most common damage is circular or elliptical in shape, as shown in figure 2 (b), and is more conducive to calculating an accurate POD. This limitation has made it difficult for SHM system designers to accurately predict POD, thus compelling them to either over-design the number of sensors needed or base their design on extensive laboratory testing. During this work, we first attempted to develop a model to predict the POD of an elastic wave based SHM system on metallic sheets. However, we realized that we did not have access to the resources needed and decided to perform an experiment to estimate the POD.

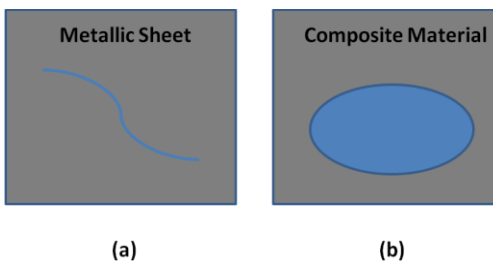


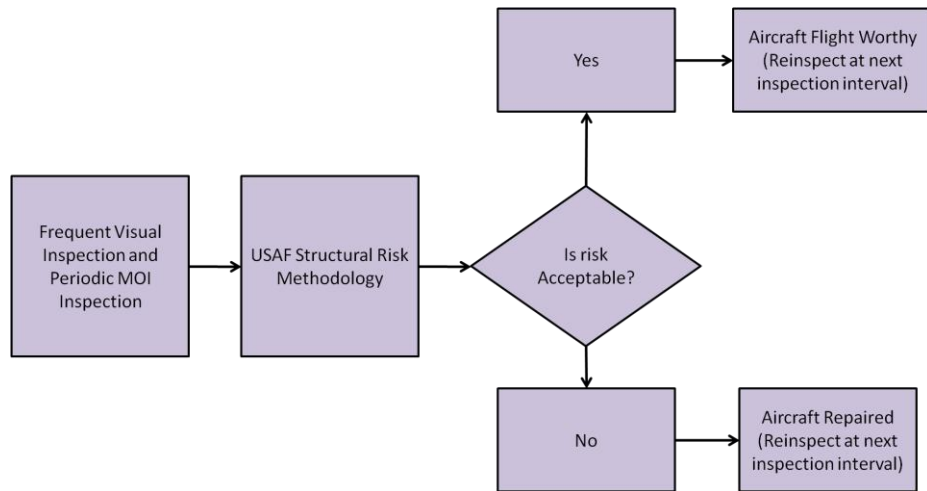
Figure 2. Most common types of damage for (a) metallic sheets (b) composite materials

1.4 Specific Objectives

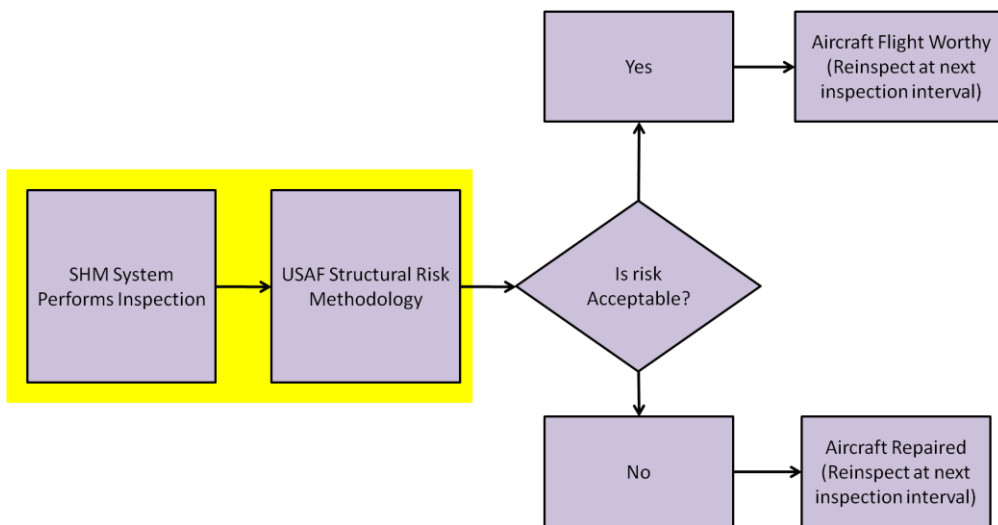
The goal of this thesis was to investigate the extension of the USAF Structural Risk Methodology to perform a risk analysis using the input from two different SHM systems on a portion of a cargo aircraft's frame (P. Hovey A. B., 1998). Our goal was to investigate combining COTS SHM systems, an elastic wave based system and an eddy-current system, with the USAF Structural Risk Methodology and quantify the resulting lifetime risk of the proposed system. Figure 3 shows both the current risk analysis system, which uses frequent visual inspections and periodic MOI inspections and our proposed system where our proposed changes are highlighted in yellow. In order to accomplish this objective, we performed several tasks that will be discussed in the subsequent sections and are listed below.

1. Discuss the function of an elastic wave and an eddy-current SHM system.
2. Provide an in-depth definition of POD for an integrated SHM system.

3. Discuss USAF Structural Risk Methodology.
4. Perform a risk-analysis for both an elastic wave and an eddy current SHM system, including a single flight probability of failure (SFPOF) analysis.



(a)



(b)

Figure 3 (a) Current Air Force risk analysis process (b) Proposed risk analysis process with changes highlighted in yellow

CHAPTER 2

SHM SYSTEMS

2.1 Elastic Wave Based SHM Systems

Piezoelectric SHM systems, also known as elastic wave based SHM systems, are one the most widely used SHM systems (S. Bo-Lin, 2008). A piezoelectric SHM system uses the propagation of elastic waves through a material and measures this against a baseline measurement to detect damage present on the structure. The piezoelectric sensors measure the elastic waves via the piezoelectric effect in which a mechanical vibration causes a change in the electrical polarization, resulting in a subsequent voltage change across the piezoelectric material (S. Bo-Lin, 2008; Y. Lu, 2009). Piezoelectric systems are attractive for SHM applications because the piezoelectric transducers can act as both a passive and active measurement systems. In a passive mode, the piezoelectric actuators listen for unexpected elastic waves propagating in the airframe that could be caused by something impacting the airframe or by crack growth events, as shown in figure 4 (a) (S. Bearda, 2005). In active mode, one of the piezoelectric transducers is used to create the elastic wave and the other transducers listen to the resulting wave to detect damage present in the airframe, illustrated in figure 4 (b) (S. Bearda, 2005).

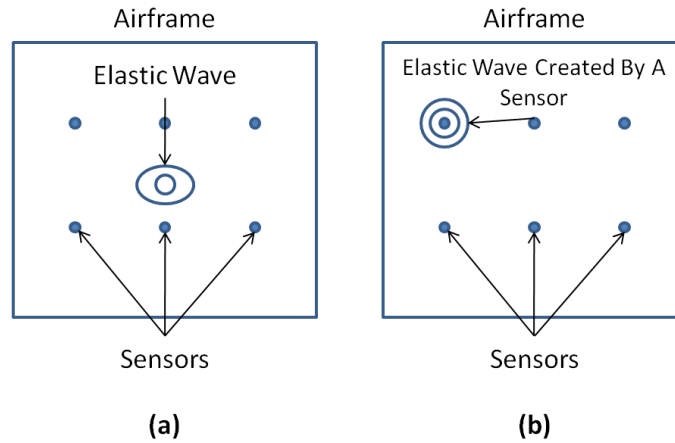


Figure 4. (a) Passive piezoelectric SHM system (b) Active piezoelectric SHM system

In passive mode, the piezoelectric SHM system uses the data collected from multiple sensors to determine location and amplitude of the impact or fracture event. This is done by calculating the difference of time of arrival of the elastic waves to the various sensors and by looking at the difference in the measured amplitude of the impact, as shown in figure 5 (S. Beard, 2007).

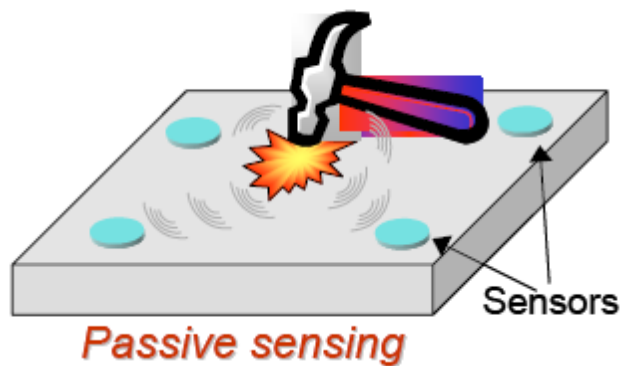


Figure 5. Passive SHM System (S. Beard, 2007)

In active mode, the SHM system uses a transducer to create an elastic wave in the structure and then measures the response via the path between the active transducer and the remaining sensors (S. Beard, 2007). Figure 6 depicts an active SHM system.

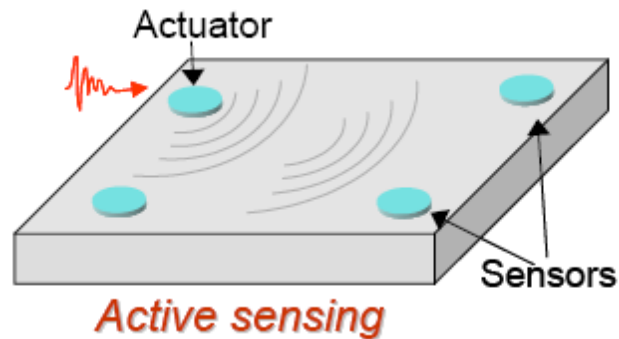


Figure 6. Active SHM System (S. Beard, 2007)

A commercially available system by Accelent embeds piezoelectric sensors on a thin layer of material called the SMART Layer® (S. Bearda, 2005). This allows for easy integration of a large number of sensors (S. Bearda, 2005).

The SMART Layer® is well established in the field of Structural Health monitoring and provides a wider structural coverage for gathering data than a similar system where each sensor must be installed individually (S. Bearda, 2005). The layer is made from a network of distributed PZT (lead-zirconate-titanate) piezoelectric disc transducers that are embedded in the SMART Layer® and act as both sensors and actuators for monitoring the health of a structure in real-time (S. Bearda, 2005). The SMART Layer® manufacturing process utilizes the printed circuit technique in order to connect a large number of sensors embedded in the layer without requiring individual connections to be made manually (S. Bearda, 2005). The SMART Layer® is thin, very lightweight, and provides excellent electrical insulation allowing the system to be used on metallic airframes (S. Bearda, 2005). The SMART Layer® can be bonded onto metal surfaces using epoxy making them easy to install (S. Bearda, 2005).

2.2 POD Of Smart-Layer SHM System

Due to the inherent difficulties of calculating POD on a thin sheet of metal discussed earlier, an experiment was developed using MIL-HBK 1823-A guidelines (Department of Defense, 2009). Before the

experiment was conducted, the parameters that affect the POD were determined such as; flaw size, geometry, and material properties. During the experiment we were primarily concerned with an aluminum sheet, thus a representative sample of a cargo plane was used as a test article, as shown in figure 7.

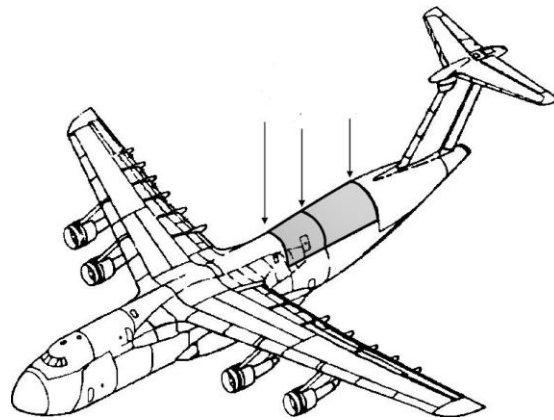


Figure 7. Illustration of cargo plane showing where sample was taken from

Two 4 frame wide by 7 frame long panels were chosen in order to test both SHM systems and the results were used to estimate their POD, like the frame shown figure 8. For the test, SHM sensors were designed and installed to monitor the four bays enclosed in the red box of figure 8. For the sake of time, the structure was not subjected to any static or cyclical loading. Instead, a Dremel tool was used to cut cracks of various orientations and sizes. These cracks were meant to simulate cracks through the metallic sheet, similar to those that would be experienced throughout the aircraft's lifetime.



Figure 8. Test Subject was 4 frame wide by 7 frame panel (red box specifies test area)

2.2.1 Piezoelectric SHM System Experiment

In order to install the piezoelectric SHM system, the surface of the metallic sheet was first cleaned off with a solvent. The surface was then slightly “roughened” using sandpaper and then wiped clean to remove the dust. Next, a two part epoxy adhesive was used to bond the SMART Layer® to the surface of the structure, as shown in figure 9. This adhesive provides a rigid interface between the piezoelectric elements and the structure giving the system the high mechanical coupling needed to transmit strain between the actuator/sensors and the structure.

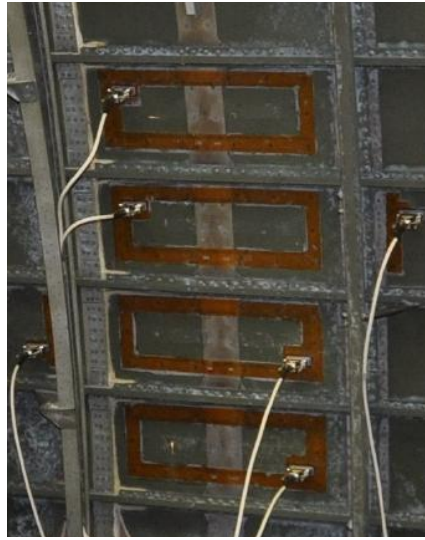


Figure 9. Piezoelectric SHM setup

Heat lamps were used to attempt to speed up the curing process. However the metallic sheet acted as a gigantic heat sink, making it difficult to keep the temperature high enough to cure the epoxy adhesive. After limited success, the epoxy was allowed to cure overnight before testing began.

For redundancy, excess piezoelectric sensors were used. This allowed us to get the most information out of testing. In addition, the SHM software allows for the data from various sensors to be removed during post-processing allowing us to see the effects on POD of less dense configurations. The sensor/actuator signal paths are shown in figure 10. The actuator input that is used to excite the piezoelectric elements is a 5-peak modulated sine wave, shown in figure 11. Signals were generated for each path at 250 kHz and 350 kHz and a typical sensor response is shown in figure 12.

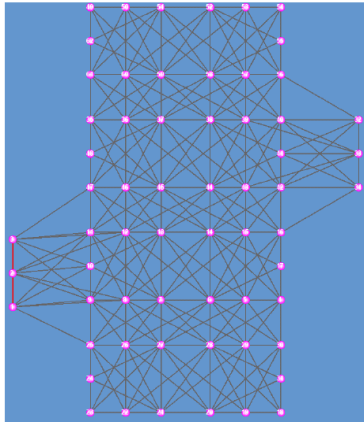


Figure 10. Signal/sensor paths of piezoelectric SHM system

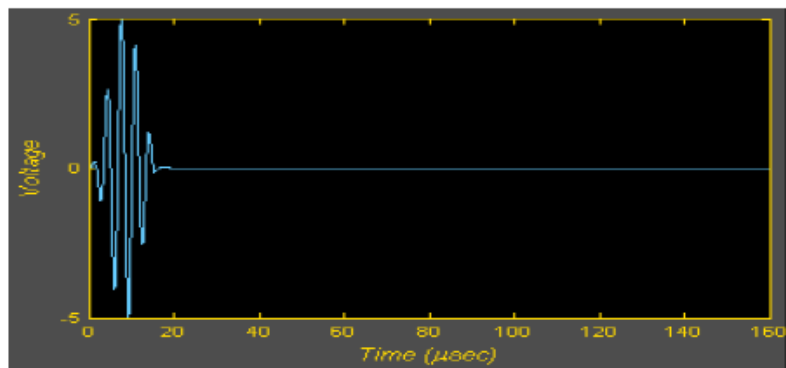


Figure 11. 5-peak modulated sine wave used to excite piezoelectric actuator

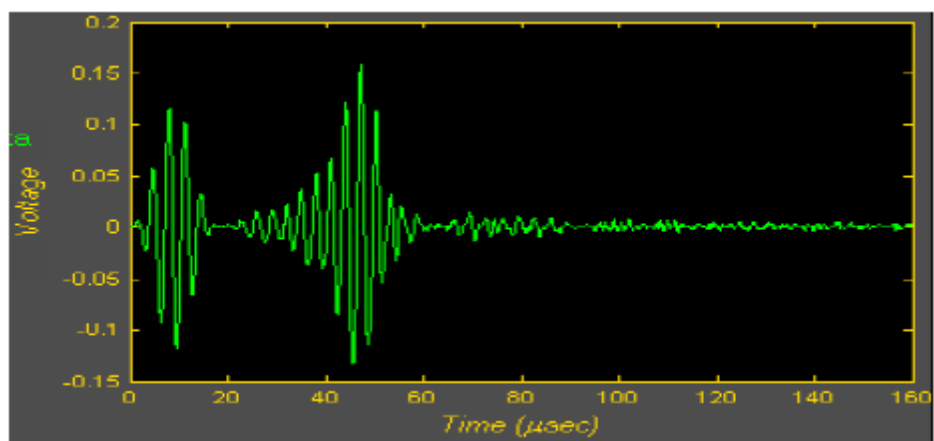


Figure 12. Typical piezoelectric sensor response

To prepare for testing, a baseline measurement of the entire system was taken at various temperatures to allow for temperature correction. After the baseline had been established, the Dremel Tool was used to create simulated cracks. After a crack had been added, the SHM system performed an inspection and the results were archived. All in all, six types of cracks were created on the structure; types T1 and T2 are circumferential cracks between fasteners under the frames, T3 is a circumferential crack between fasteners under a stringer, T4 is an axial crack under a stringer, T5 is a circumferential crack within a bay, and T6 is an axial crack within a bay. During the testing, 12 artificial cracks of the types T1 through T6 were introduced at various locations. A pictorial representation of each type of crack is shown in figure 13.

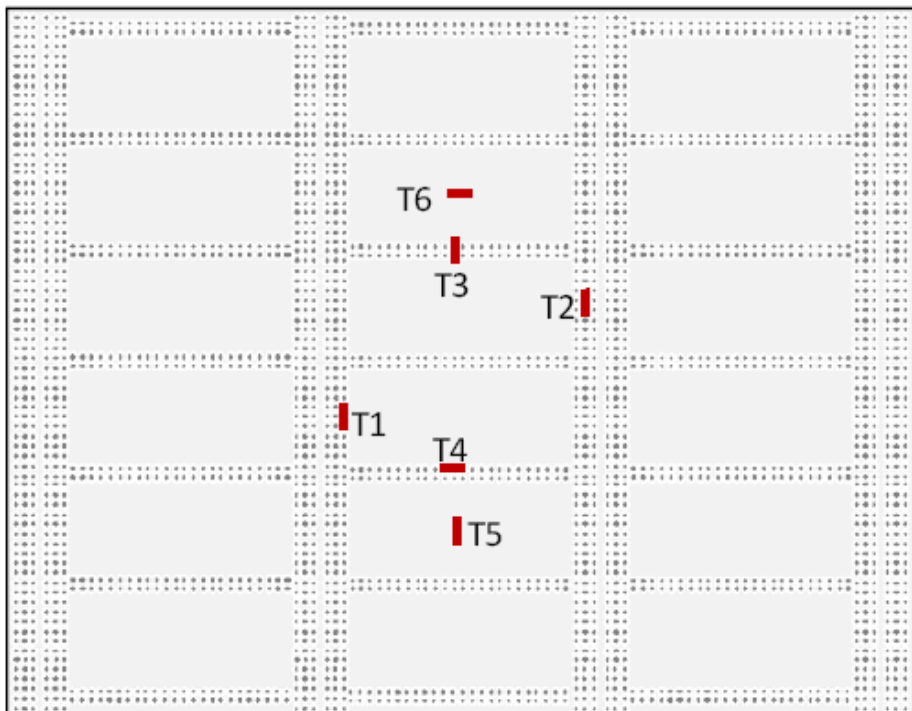


Figure 13. Location and orientation of twelve cracks added to the airframe

After each flaw was added, data was collected and the SHM system was triggered to inspect the airframe. The piezoelectric SHM system compares the sensor responses of the system with the previous baseline response of the undamaged structure to determine if damage is present. Thus, the difference between the two responses contains the information about any damage of the structure.

In this experiment, two piezoelectric SHM analysis methods were used. The first method determines the total amount of energy in each sensor path and creates a 2-D mapping of the structure. This method, referred to as Direct Path Image, provides a quick visual representation of the location of structural changes and was used during the demonstration (S. Beard, 2007).

The second method utilizes the wave velocities of the S_0 and A_0 Lamb wave modes in each sensor/actuator path to extract the reflectance of each signal and generate a resulting diagnostics image (S. Beard, 2007). This technique, Reflection Based Analysis (RBA), produces more accurate representations for single crack damage (S. Beard, 2007). However, RBA has more difficulty when several cracks are near each other because of the multiple reflections (S. Beard, 2007).

Prior to any damage being induced, a no damage set of data was taken. Figure 14 shows the no damage (blue) mapping of the structure.

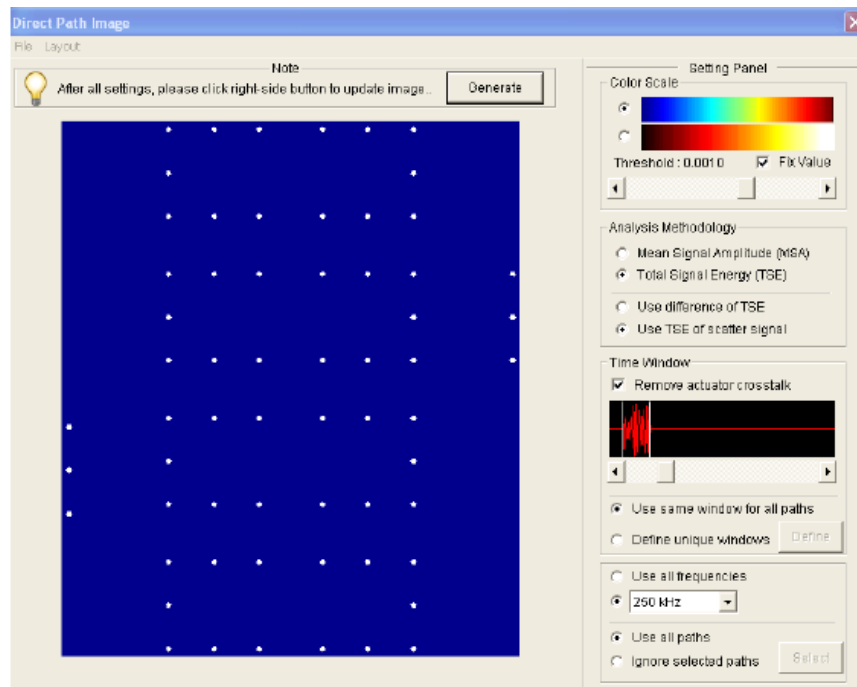


Figure 14. Diagnostics image of the no-damage baseline configuration

The first damage that was induced was a type T5 circumferential crack within a bay that was located on the left hand side of the bottom bay. Using the Direct Path analysis, the crack was detected. However, it should be noted that the detected location of the crack was off by a few inches. Figure 15 shows the Direct Path image created by the system. The actual location of the crack is shown as a vertical yellow strip. In addition, the RBA analysis also detected crack 1. In fact, the RBA analysis was much more accurate and is expected for a single flaw situation like this. Figure 16 shows the RBA image generated. Notice the flaw is detected right where the actual crack is located.

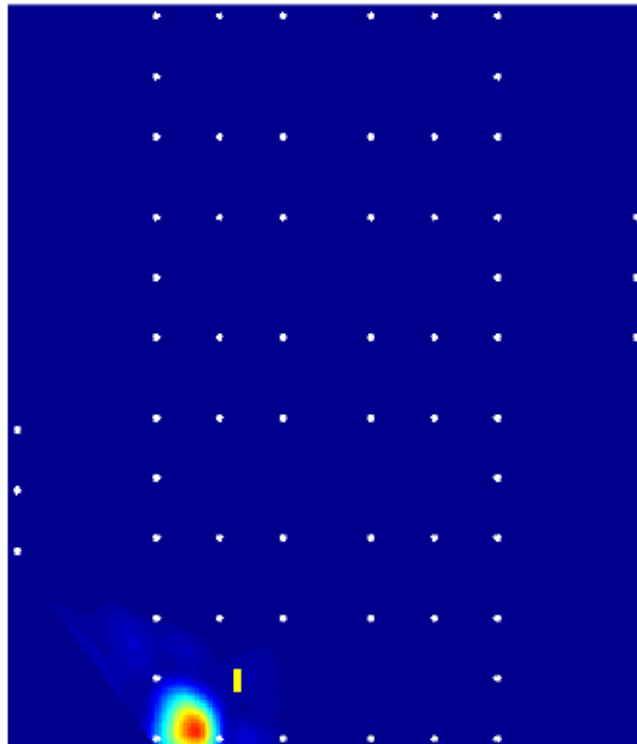


Figure 15. Direct Path image for crack 1

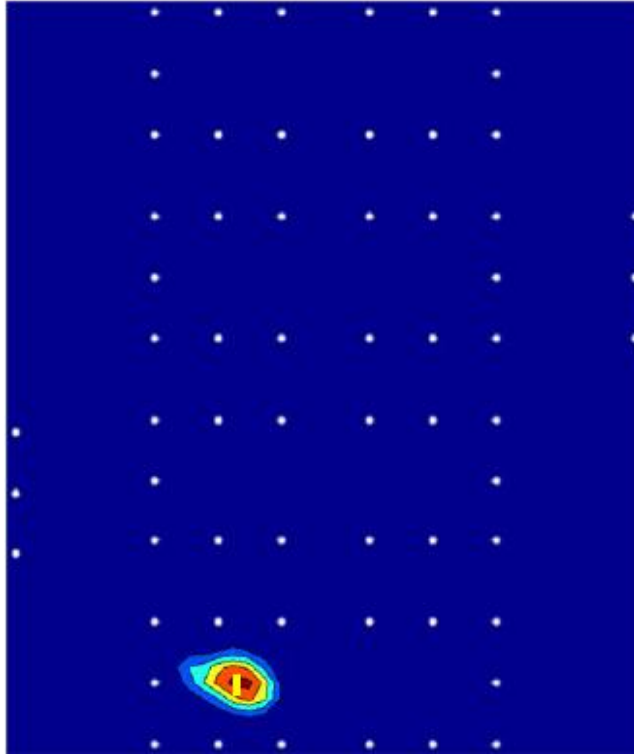


Figure 16. RBA image for crack 1

The second flaw introduced was type T3 circumferential crack between fasteners under a stringer. This crack was located on the edge of the sensor network directly in line on the path between two sensors. Since the crack is parallel with the sensor/actuator path going directly through it, the signal for the path is relatively unaffected. Figure 17 shows the Direct Path image where the damage does not show up. By increasing the sensitivity, the Direct Path image is capable of resolving the damage, seen in figure 18. However, the increased sensitivity can lead to false positives. The red lines in figure 18 show the sensor paths that detected damage. Notice, that the lower far left sensor paths detected damage when none was present. Using the RBA analysis, crack 2 is easily detected and located, as shown in figure 19.

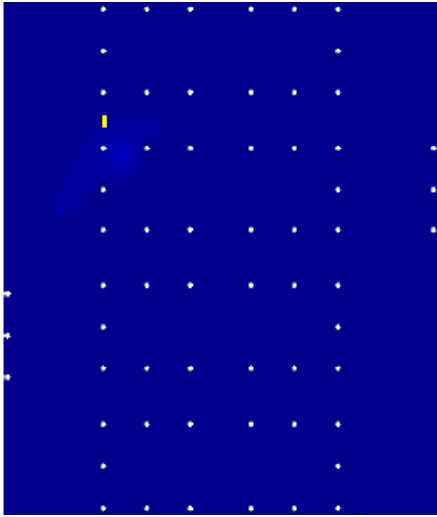


Figure 17. Initial Direct Path image for crack 2

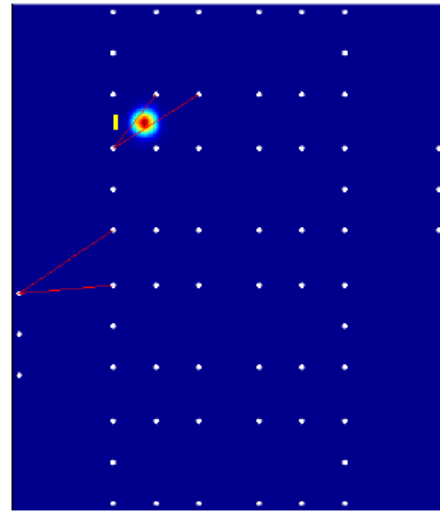


Figure 18. Direct Path image of crack 2 with increased sensitivity

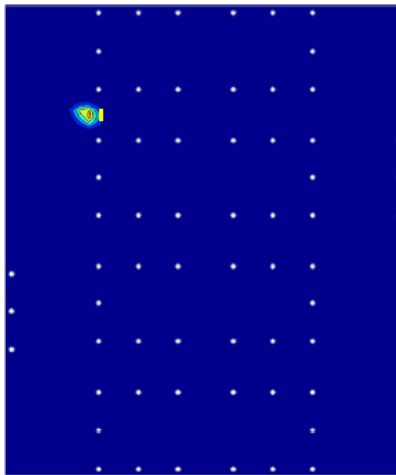


Figure 19. RBA analysis image of the crack 2

Using the Direct Path method, multiple flaws can be detected and imaged. Figure 20 shows both crack 2 and crack 3, which are both T3 circumferential cracks between fasteners under a stringer that are located near each other. In addition, figure 21 shows cracks 2-6.

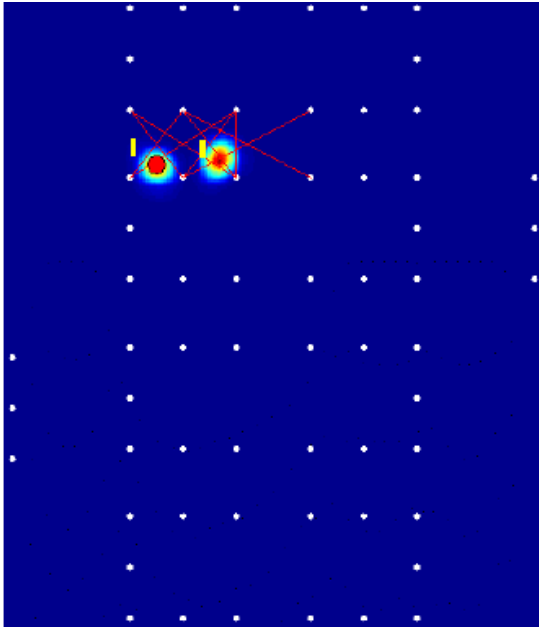


Figure 20. Direct Path image of crack 2 and crack 3

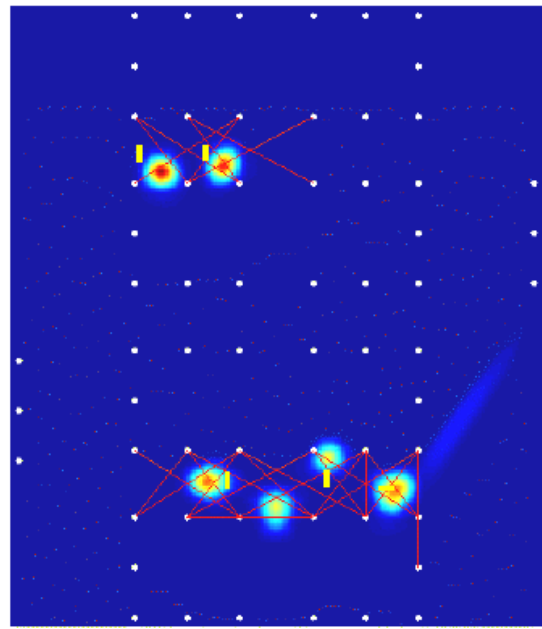


Figure 21. Direct Path image of cracks 2-6

All in all, twelve cracks were introduced to the structure. Both methods, Direct Path and RBA, were used to analyze the flaws. Table 2 shows the results for each flaw using both methods. The Direct Path Image method had difficulties detecting damage on the edges of the sensor layout such as; crack 2, crack 9, and crack 10. The Reflection Based Analysis could detect cracks everywhere including the edges of the sensor layout. However, RBA had difficulties imaging multiple cracks that were near each other. Since the RBA analysis detected there was damage and the only problem was its inability to resolve individual cracks, each crack was counted as a positive detection. In its real application, a combination of both techniques would be used to detect cracks present on the structure and since we are primarily worried with POD we will not distinguish between which analyses detected the crack.

Table 2. Experimental results for piezoelectric SHM POD test

Crack Number	Direct Path (Y=Detected N=Not Detected)	RBA (Y=Detected N=Not Detected)
1	Y	Y
2	N	Y
3	Y	Y
4	Y	Y
5	Y	Y
6	Y	Y
7	Y	Y
8	Y	Y
9	N	Y
10	N	Y
11	Y	Y
12	Y	Y

In order to estimate POD for the piezoelectric SHM system, the methods outlined in MIL-HBK-1823A Hit/Miss Analysis will be used. First, a log odds distribution is assumed (Department of Defense, 2009; A.F. Grandt, 2004). In order to estimate POD, the ratio of hits to misses is needed. In addition, a 50% flaw size, $a_{50\%}$, is needed and corresponds to the crack size, a , that is detected by the SHM system 50% of the time. Also, the smallest detectable crack size distinguishable from noise, a_{th} , and the standard deviation must be specified. Due to limitations of resources, the size of the experimental data set is inadequate to develop an accurate POD curve. Thus, the value of the parameters selected and the logic behind their selection will be discussed.

For the sake of the analysis, we tried to maintain a conservative viewpoint with respect to the POD of the SHM system. Thus, all twelve holes will be considered to be the same size that will be estimated to be one inch. The POD will be specified for each crack size and notated as a proportion of the size in inches. Since the SHM system was able to detect all 12 cracks the hit/miss ratio will be classified as 1. However to keep a conservative viewpoint, the 50% size will be considered to be 0.95 inches. Taking into consideration that the holes were drilled manually, this should be very conservative because the variance of the holes was likely more than +/- 5% and the simulated cracks were still detected. To estimate the value For a_{th} , the minimum value detectable flaw size of an ultrasonic system 0.07 inches, shown in table 1, will be used. Since the data set is small, we will use a high standard deviation of 0.5 inches.

The POD model can be expressed mathematically using the following derivation. For hit/miss testing, the likelihood of P, based on a single observation, is:

$$L(P_i, a_i, x_i) = P_i^{x_i}(1 - P_i)^{1-x_i} \quad (\text{Eq 3.1}) \quad (\text{J.P. Gallagher, 1984})$$

where P_i is the probability of detection of crack size a_i , x_i is the inspection outcome, 0 for miss, 1 for hit. (Notice that when the exponent of $P_i^{x_i}$, is one, that of $(1 - P_i)$ is zero, and so that factor, $(1 - P_i)^0$, reduces to multiplication by one. Similarly with $P_i^{x_i}$, when x is zero. P_i is a function of crack size, a_i , and the log normal model can be used to relate $P_i = \text{POD}(a_i)$ with crack size (J.P. Gallagher, 1984). The model formulation is

$$P_i = \text{POD}(a_i) = 1 - Q(z_i) \quad (\text{Eq 3.2})$$

where $Q(z)$ is the standard normal survivor function, $z_i = \log \left[\frac{a_i - \mu}{\sigma} \right]$ is the standard normal variate, m, s are the location and scale parameters (J.P. Gallagher, 1984). Using Microsoft Excel, the POD was calculated for an index of crack numbers. Figure 22 shows the calculated POD for the piezoelectric SHM system that will be used with the USAF Structural Risk Methodology.

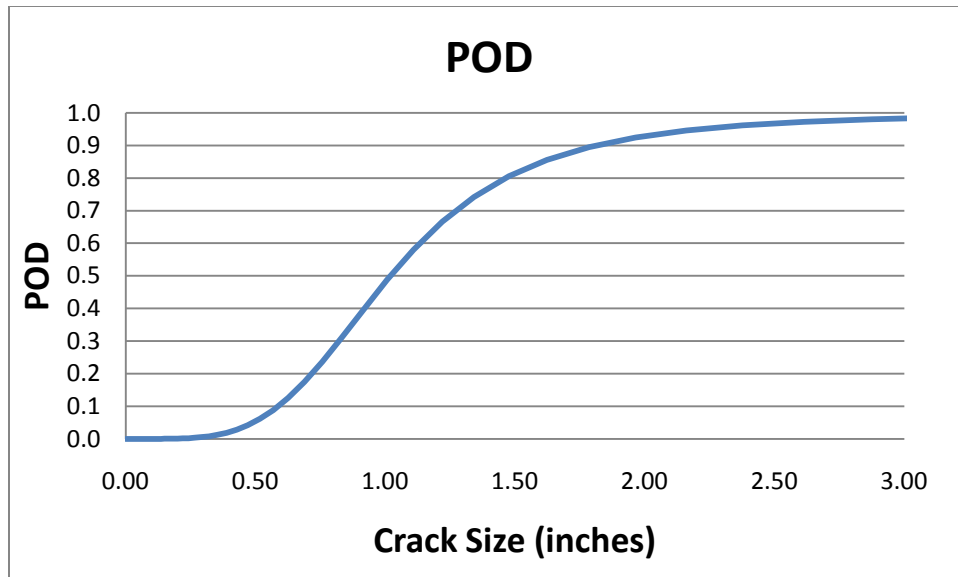


Figure 22. Plot of calculated POD for piezoelectric SHM system

2.3 Eddy Current SHM Systems

Eddy Current SHM (ECSHM) Systems, also known as meandering winding magnetometers (MWM®), use surface mounted periodic field eddy-current MWM-Arrays to detect cracks and monitor crack growth in real-time (N. Goldfine, 2002). These MWM-Arrays can be surface mounted, like the inside of a fuel tank for example, placed around fasteners and in-between layers such as a lap joint (N. Goldfine, 2002). Eddy current testing allows the inspection of surface-breaking as well as subsurface discontinuities, which are not too deep due to skin effect (R. Grimberg, 2005). Figure 23 shows a 2 channel and 7 channel MWM eddy current sensor.

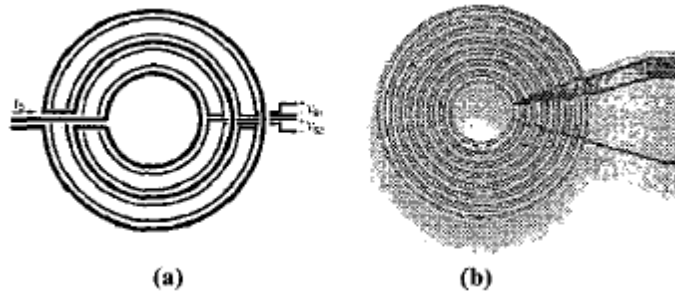


Figure 23. (a) 2 channel MWM array (b) 7 channel MWM Array (N. Goldfine, 2002)

A Surface mountable MWM-Rosette, as shown in figure 23, is an example of a sensor design suitable for surface mounting on aircraft (N. Goldfine, 2002). When designing surface mountable MWM Arrays, three key requirements must be taken into consideration. First, the sensing footprint must be large enough to cover the area of interest. Second, the resolution of the sensing elements must be sufficient to detect the smallest defect that must be distinguished. Last, at least one element should be placed in a region not likely to contain cracks during the inspection period.

Several factors affect the POD of an ECSHM system; however the frequency of the eddy current plays the largest role in the probability of detection of flaws that are located below the surface (R. Grimberg, 2005). For subsurface defects, a low frequency eddy current is desirable to achieve an acceptable POD (R. Grimberg, 2005). However, a low frequency eddy current, when implemented, reduces the sensitivity of the eddy current signal making it necessary for sophisticated signal processing and inversion methods (R. Grimberg, 2005). Inversion methods allow for the determination of the defect's size, position, and even the shape (R. Grimberg, 2005).

2.4 POD Of Eddy-Current SHM System

Due to limitations on resources, we were not able to perform an experiment with the eddy-current SHM system. Instead, it was decided to use typical POD data for an eddy-current SHM system (Peil, 2003; Sindel, 1998). Estimating data points from the plot, the value of $a_{50\%}$ was estimated to be 1.5 mm or 0.06 inches. The value of a_{th} was estimated to be 0.5 mm or 0.02 inches. The standard deviation was

assumed to be 1 mm or 0.04 inches. Using the same hit/miss model used on the piezoelectric SHM system, the POD plot shown in figure 24 was calculated.

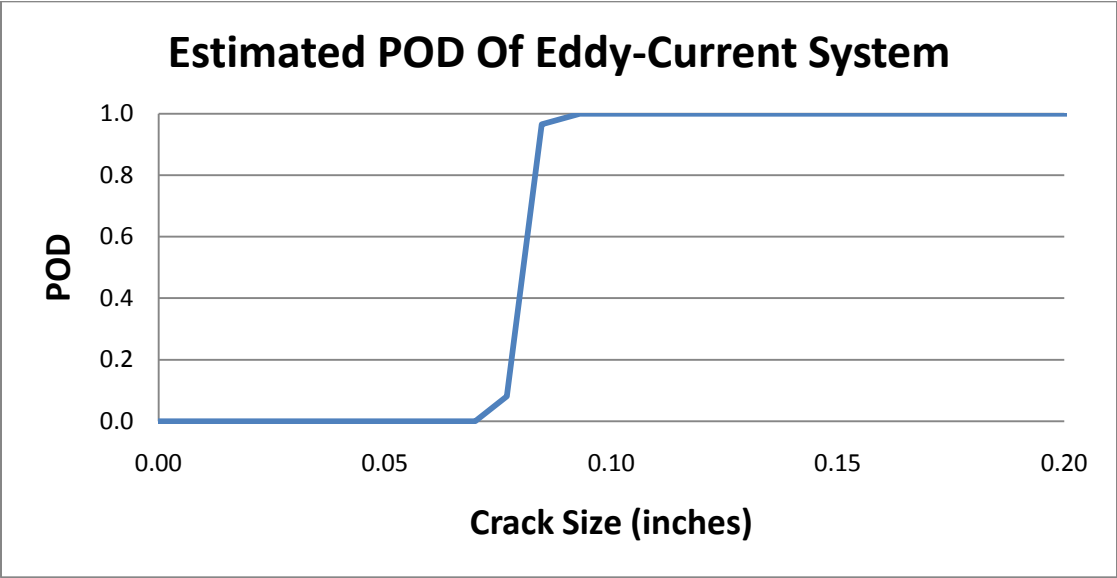


Figure 24. Estimated POD for eddy current SHM system (Peil, 2003; Sindel, 1998).

CHAPTER 3

USAF STRUCTURAL RISK METHODOLOGY

3.1 Structural Risk Analysis

The Air Force ensures structural integrity of its fleets by manual inspections based on the model of the growth of discrete cracks that are assumed to be present in the structure (P. Hovey A. B., 1998). Additional structural risk analysis has been used to provide a better understanding of the risks of stochastic element failure (P. Hovey A. B., 1998; Berens, 1996). This information has been used for determination of inspection intervals and maintenance procedures (P. Hovey A. B., 1998; Berens, 1996).

PROF (Probability Of Fracture) was written to facilitate the Air Force implementation of structural risk analysis (P. Hovey A. B., 1998; Berens, 1996). Structural risk analysis is a fleet management tool that is used for decisions regarding the timing and extent of inspection, repair, or replacement maintenance on structures (P. Hovey A. B., 1998; Berens, 1996). It is based on the POF of a structure within a fleet. In a fatigue environment, the strength and stress relationship is dynamic because the strength of the structure degrades as defects grow on it (P. Hovey A. B., 1998; Berens, 1996). Fracture mechanics provides a probabilistic model to predict the growth of cracks for a given stress distribution and initial flaw size (P. Hovey A. B., 1998; Berens, 1996).

The output of PROF is a probabilistic distribution that predicts the risk of a failure of a structure (P. Hovey A. B., 1998; Berens, 1996). This distribution is then used to make maintenance decisions. The Failure risk associated with the growth of cracks in a structure is dependent on the crack size, loads experienced during flight, geometry of the aircraft, the scatter in the material properties, the interval time between inspections, and the detection capabilities of the inspection process (P. Hovey A. B., 1998; Berens, 1996). PROF provides the probabilistic risk for a structure with a single crack of size, a , using the Irwin Fracture Criterion (P. Hovey A. B., 1998; Berens, 1996).

Since PROF has been released other damage scenarios found on aging aircraft have been identified and investigated; including discrete source damage (DSD) in the presence of multi-site damage (MSD), wide-spread fatigue damage (WFD), and potential effects of corrosive thinning in a fleet (P. Hovey A. B., 1998; Berens, 1996). In order to provide these capabilities, WINPROF was created. WINPROF has three additional capabilities that were added to address the issues (P. Hovey A. B., 1998; Berens, 1996). The first capability added was probabilistic risk assessment of discrete source damage (P. Hovey A. B., 1998; Berens, 1996). In addition, a multi-run data management capability was added. Finally, the windows graphical user interface (GUI) was improved and the POF calculations were improved also (P. Hovey A. B., 1998; Berens, 1996).

The DSD problem is related to the ability of a structural member to perform its function in reaction to an adjacent structural member failing (P. Hovey A. B., 1998; Berens, 1996). The presence of MSD could degrade the ability of a structure to carry the additional load when a DSD occurs (P. Hovey A. B., 1998; Berens, 1996). The emphasis of the DSD problem is the conditional probability of a failure in the structure; given the failure of the adjacent structure has occurred (P. Hovey A. B., 1998; Berens, 1996). In a DSD problem, the situation is modeled the same until the DSD event occurs and then the fracture criterion is changed (P. Hovey A. B., 1998; Berens, 1996). The shifting of the load due to an adjacent structure element is complex and is not modeled well using the Irwin abrupt fracture criteria, thus a change in the criteria was needed (P. Hovey A. B., 1998; Berens, 1996).

Since a single run of PROF produces the POF of a structural element as a function of flight hours for a specific loading, crack distribution, material properties, and geometry; several PROF analyses would be needed to determine POF for an entire aircraft (P. Hovey A. B., 1998; Berens, 1996). A WINPROF interface to Microsoft Excel was added to allow for multi-run data management more easily and thus allow more complex systems to be analyzed (P. Hovey A. B., 1998; Berens, 1996).

3.2 USAF Structural Risk Model

Fracture of a structure occurs when an applied stress produces a stress intensity factor that exceeds the fracture toughness of the material (P. Hovey A. B., 1998; Berens, 1996; P. Hovey J. G., 1983). This relationship is shown in equation 3.1,

$$\sigma \geq \sigma_c = \frac{K_c}{\sqrt{\pi a} \beta(a)} \quad (\text{Eq. 3.3}) \quad (\text{P. Hovey A. B., 1998})$$

where σ is the stress intensity, σ_c is the maximum normal stress allowed in the critical plane, a is the crack size, K_c is the fracture toughness of the material, and $\beta(a)$ is a geometry dependent factor (P. Hovey A. B., 1998; Berens, 1996; P. Hovey J. G., 1983; P. Hovey J. G., 1983). Thus the probability of fracture (POF) can be defined as the probability that the max stress experienced during flight is greater than the maximum allowable stress in flight

$$POF = P\{\sigma_{max} \geq \sigma_c\} \quad (\text{Eq. 3.4}) \quad (\text{P. Hovey A. B., 1998})$$

In the case of the POF as a function of the growth of a single crack, equation 3.1 can be rearranged as

$$\frac{K}{\sigma} = \sqrt{\pi a} \beta(a) \quad (\text{Eq. 3.5}) \quad (\text{P. Hovey A. B., 1998})$$

Equation 3.3 is the defining relationship between stress intensity factor, stress, and crack size (P. Hovey A. B., 1998). In order to calculate POF, probabilistic models for the crack-size, fracture-toughness, and stress exceedance are used (P. Hovey A. B., 1998). The POF can then be expressed as

$$POF = \int_0^{a_c} f(a) \int_0^{\infty} g(K_c) \hat{H}(\sigma_c(aK_c)) dK_c da + [1 - F(a_c)] \quad (\text{Eq. 3.6}) \quad (\text{P. Hovey A. B., 1998})$$

where $f(a)$ is the crack-size probability density function, $g(K_c)$ is the fracture-toughness probability density function, $\hat{H}(\sigma) = 1 - H(\sigma)$ is the exceedance probability distribution function for the peak stress in a single flight, and $\sigma_c(aK_c)$ is the critical stress for the given crack size and fracture toughness (P. Hovey A. B., 1998). A normal probability density function can be used to model the fracture-toughness probability density function $g(K_c)$ as shown in equation 3.5,

$$g(K_c) = \frac{1}{\sigma\sqrt{2\pi}} e^{-\frac{(x-\mu)^2}{2\sigma^2}} \quad (\text{Eq. 3.7}) \quad (\text{P. Hovey A. B., 1998})$$

where μ is the mean and σ^2 is the variance (P. Hovey A. B., 1998; W. Hines, 2003; Leon-Garcia, 2008; Ross, 2004).

A Gumbel type 1 distribution is used to model the distribution of the maximum stress per flight. A Gumbel type 1 distribution is the most common type of Fischer-Tippett extreme value distribution (Weisstein; Gumbel E. J., 1960; Gumbel E. , 1961). The Gumbel Type 1 distribution is an extreme order statistic for a distribution of N elements X_i and is used to refer to the distribution corresponding to a minimum extreme value distribution, the distribution of the minimum $X^{(i)}$ (22-24). The Gumbel distribution has the general form;

$$P(x) = \frac{1}{\beta} \exp \left[\frac{x-\alpha}{\beta} - \exp \left(\frac{x-\alpha}{\beta} \right) \right] \quad (\text{Eq. 3.8})$$

$$D(x) = 1 - \exp \left[-\exp \left(\frac{x-\alpha}{\beta} \right) \right] \quad (\text{Eq. 3.9})$$

where $P(x)$ is the probability density function and $D(x)$ is the distribution function (Weisstein; Gumbel E. J., 1960; Gumbel E. , 1961).

In the case of maximum stress per flight it can be written as;

$$P\{\sigma_{max} \geq \sigma\} = \check{H}(\sigma) = 1 - \exp \left[-\exp \left(-\frac{\sigma-B}{A} \right) \right] \quad (\text{Eq. 3.10}) \quad (\text{P. Hovey A. B., 1998})$$

where A and B are mission parameters that must be supplied by the user (P. Hovey A. B., 1998).

The POF calculation can then be simplified to

$$POF = \int_0^{a_c} f(a) POF(a) da + [1 - F(a_c)] \quad (\text{Eq. 3.11}) \quad (\text{P. Hovey A. B., 1998})$$

In the case of calculating POF as a function of a specified crack size, a, equation 3.9 can be expressed as (P. Hovey A. B., 1998);

$$POF(a) = \int_0^{\infty} g(K_c) \hat{H}(\sigma_c(aK_c)) dK_c \quad (\text{Eq. 3.12}) \quad (\text{P. Hovey A. B., 1998})$$

Equation 3.10 is the analytical formula for determining POF, however the numerical solution to this equation is vulnerable to errors because $f(a)$ cannot be determined explicitly (P. Hovey A. B., 1998). Instead, $f(a)$ must be determined from a look up table of values of the cumulative probability distribution function $F(a)$ (P. Hovey A. B., 1998). To get around this, a change of variable is used such that $F(a)$ is used rather than $f(a)$. To do this, we take advantage of the fact that for any uniform random variable u on the interval $(0,1)$ $x = F^{-1}(u)$ has the distribution function $F(x)$ (P. Hovey A. B., 1998). Equation 3.10 can then be rewritten as

$$POF(a) = \int_0^{a_c} POF(F^{-1}(u)) du + [1 - F(a)] \quad (\text{Eq. 3.13}) \quad (\text{P. Hovey A. B., 1998})$$

The previous equations describe the probability of fracture as a function of crack size. However, we are primarily interested in the probability of failure during flight. Currently, we are calculating a single-flight structure probability of failure as the sum of the probability of fracture during the current flight plus the probability that the crack size present on the structure exceeds the critical crack size just prior to flight (P. Hovey A. B., 1998). This can be expressed as

$$P_f = \int_0^{a_c} f(a) POF(a) da + [1 - F(a_c)] \quad (\text{Eq. 3.14}) \quad (\text{P. Hovey A. B., 1998})$$

For the case that the maximum crack size in the growth crack distribution table is less than the critical crack size, the probability of failure is the sum of the terms shown in table 1; where F_n is the last value in the crack distribution table and F_c is the extrapolated value of the crack distribution function at a_c (P. Hovey A. B., 1998).

Table 3. POF terms for case $a \leq a_c$ (P. Hovey A. B., 1998)

Interpolated Region	$\int_0^{F_n} POF(F^{-1}(u))du$
Extrapolated Region	$\int_0^{F_c} POF(F^{-1}(u))du$
Extrapolated probability that crack exceeds critical size	$1 - F_c$

For the case where the maximum crack size in the distribution table is greater than the critical crack size, F_c is interpolated and the POF is the summation of the terms in table 2 (P. Hovey A. B., 1998).

Table 4. POF terms for case $a > a_c$ (P. Hovey A. B., 1998)

Interpolated Region	$\int_0^{F_c} POF(F^{-1}(u))du$
Interpolated Probability that the crack is larger than the critical crack size	$1 - F_c$

When extrapolating the value of F_n beyond the last value in the distribution table, PROF uses the form

$$F_c(a) = 1 - \exp(-\lambda(a - \gamma)) \quad (\text{Eq. 3.15}) \quad (\text{P. Hovey A. B., 1998})$$

Equation 3.13 is linear in a plot of log of exceedance probability versus crack-length. The subsequent calculation of POF is done incrementally using the crack size distribution function $F(a)$ as

$$POF_i = \int_{F_{i-1}}^{F_i} POF(F^{-1}(u))du \quad (\text{Eq 3.16})$$

using an adaptive Romberg quadrature method (P. Hovey A. B., 1998). A final calculation from F_n to F_c is performed where $F_c = F^{-1}(a_c)$ and F_n is the value in the table less than F_c (14).

3.3 USAF Inspection And Repair Model

The USAF Structural Risk Methodology uses a probabilistic model to account for inspection and repair of a structure. For example, during an inspection a number of cracks were found and repaired. However, a crack is only found if our detection system can resolve it. In addition, each repair may not completely eliminate the crack. In order to account for this, we modify the crack size distribution at each usage interval (P. Hovey A. B., 1998). The crack size distribution is modified relative to a probabilistic model of the repair quality. This repair quality is modeled as an initial crack in the location and is subsequently used in future crack growth calculations (P. Hovey A. B., 1998).

In order to model the inspection and repair process, the process is broken down into individual pieces. When examining the inspection process, the objective is to determine the percentage of cracks, P , that are found during the inspection (P. Hovey A. B., 1998). This can be expressed as

$$P = \int_0^{\infty} POD(a)f(a)da \quad (\text{Eq 3.17})$$

where $POD(a)$ is the SHM system's probability of detecting a crack of size a , and $f(a)$ is the crack size density function before maintenance (P. Hovey A. B., 1998). This is the same POD that was calculated in section 2 for both systems.

In addition, the probability of a crack smaller than, a , can be expressed as

$$P(a) = \int_0^a POD(a)f(a)da \quad (\text{Eq 3.18}) \quad (\text{P. Hovey A. B., 1998}).$$

However, the calculation is done incrementally using the crack size distribution function $F(a)$

$$P_i(a) = \int_{F_{i-1}}^{F_i} POD(F^{-1}(u))du \quad (\text{Eq 3.19}) \quad (\text{P. Hovey A. B., 1998}).$$

The integration is done using Simpson's method with a fixed number of panels (P. Hovey A. B., 1998).

The subsequent distribution function is extrapolated from the last table value F_n using

$$F_c(a) = 1 - \exp(-\lambda(a - \gamma)) \quad (\text{Eq 3.20}) \quad (\text{P. Hovey A. B., 1998}).$$

The integral over the extrapolation region, $P_c(a)$ is calculated using the Laguerre method (P. Hovey A. B., 1998).

$$P_c(a) = \int_{a_n}^{\infty} POD(a)f(a)da \quad (\text{Eq. 3.21})$$

The quality of the repair is expressed as an equivalent repair crack size distribution $f_R(a)$ (14). By defining $f_{before}(a)$ and $f_{after}(a)$ as representing the density function of crack sizes in fleet of structures before and after maintenance action, then

$$f_{after}(a) = P * f_R(a) + [1 - POD(a)] * f_{before}(a) \quad (\text{Eq. 3.22}) \quad (\text{P. Hovey A. B., 1998}).$$

CHAPTER 4

EVALUATION STUDY OF USAF STRUCTURAL RISK METHODOLOGY BASED STRUCTURAL HEALTH MONITORING SYSTEM

In chapter 2, the structural health monitoring POD was estimated for a piezoelectric SHM system and an eddy-current SHM system. In addition, the USAF Structural Risk Analysis Model was described in chapter 3. In this chapter, both models will be combined together to test the viability of combining the USAF Structural Risk Methodology with an inspection from a COTS SHM system.

Before the feasibility of the system is discussed, the parameters used to measure the effectiveness need to be examined. First, the USAF Structural Risk Methodology is a risk-based analysis of the probability of fracture of a structure during operation, given the current state of that structure. As a result, the most important parameter is how accurately we are measuring the risk and the amount of risk at any given time. A lot of variables are used to determine the risk of the system. For this study, all other parameters discussed in chapter 3 were held constant except for the POD, which was changed for each SHM system.

For the study, a log-normal initial flaw size distribution was used with a mean, μ , equal to $3.616 * 10^{-1}$ and a standard deviation of 0.7227. Figure 25 shows the initial flaw size distribution and figure 26 shows exponential crack growth as a function of service time used during this study.

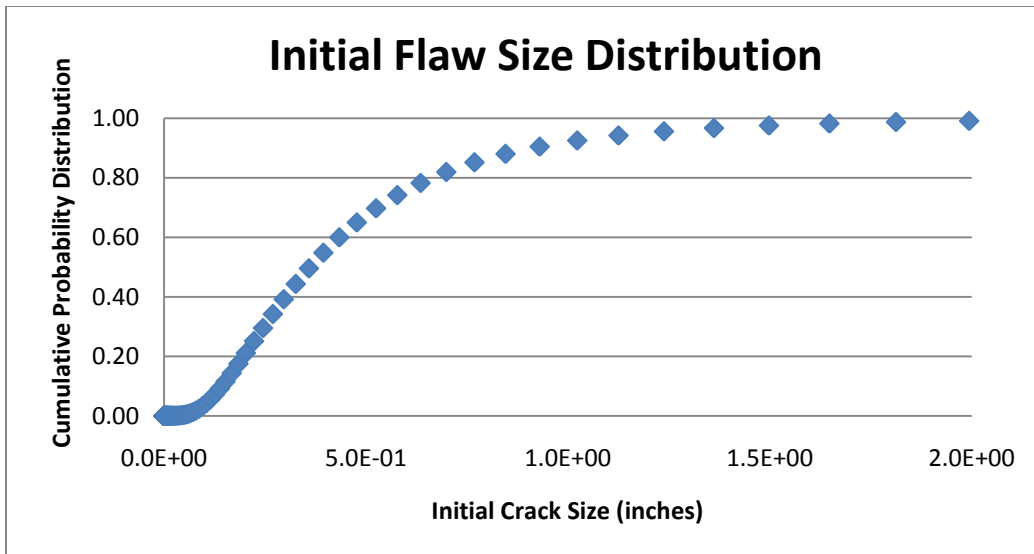


Figure 25. Initial flaw size distribution

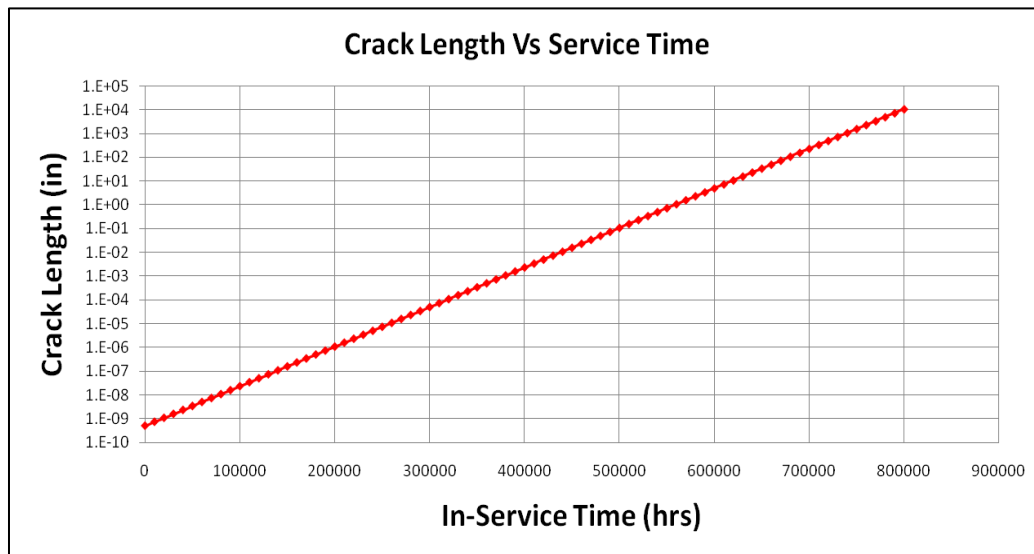


Figure 26. Crack growth as a function of service time.

The fracture toughness of the material was modeled as a normal distribution with mean of 62 $\text{ksi}\sqrt{\text{in}}$ and a standard deviation of 6.2 $\text{ksi}\sqrt{\text{in}}$. Figure 27 plots the probability density function and the cumulative distribution function of the fracture toughness.

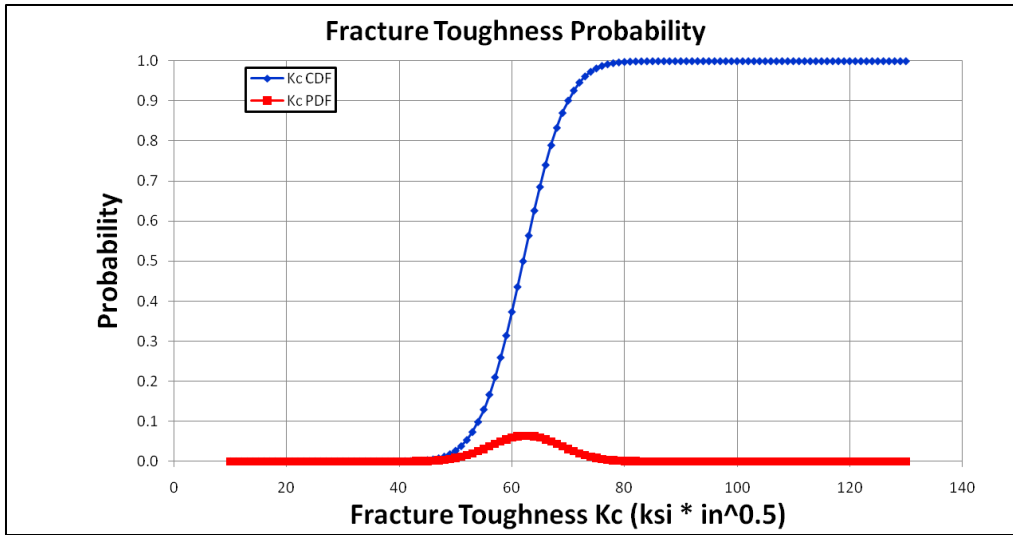


Figure 27. PDF and CDF of fracture toughness

For the stress exceedance calculation a Gumbel distribution was used where $A = 0.608$ and $B = 15.729$, as shown in Figure 28.

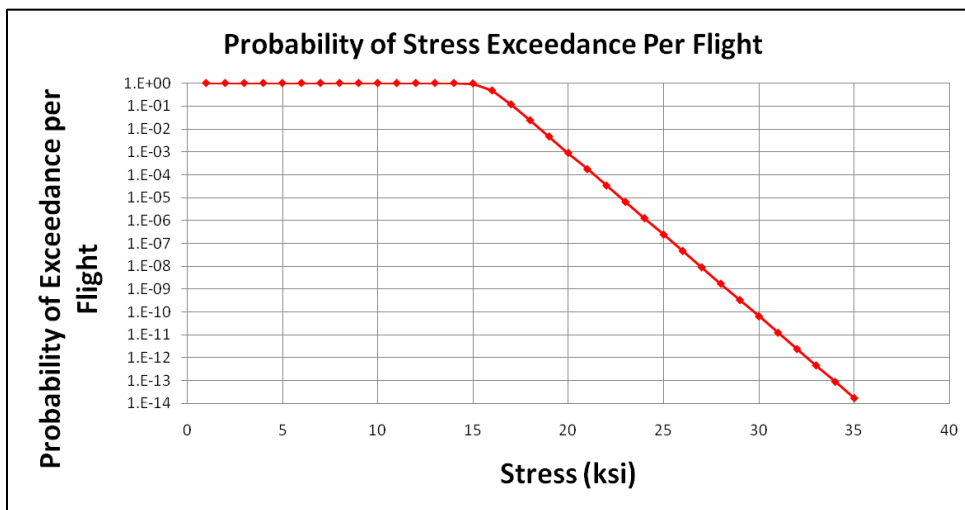


Figure 28. Probability of stress exceedance per flight

The repair process was modeled as a uniform distribution where 0.05 inches is the maximum crack size, a , that would be allowed after repair. The previous distributions will be held constant and the

USAF Structural Risk Methodology was used to estimate the single flight probability of fracture (SFPOF) for each SHM system. In order to prove the feasibility of the system, the SFPOF was calculated for each SHM system and normalized relative to the maximum allowable risk for a cargo aircraft. However, the smallest inspection period was expanded out to 365 days. The risk could have been reduced further by increasing the inspection activity; however our goal was to stay under the maximum allowable risk, while using the least amount of resources possible. Figure 29 plots the normalized SFPOF for the piezoelectric SHM system.

Notice, the single flight probability of failure never reaches the maximum allowable risk. This is a viable solution SHM system that would only require an inspection from the SHM system every 365 days. However, the total risk could be lowered if the interval between inspections were decreased. This is primarily a tradeoff between resources and could be optimized. In addition, if the system were automated such that no human resources were needed to operate the SHM system. The inspection period could be reduced dramatically, which would subsequently reduce the risk and minimize the resources needed.

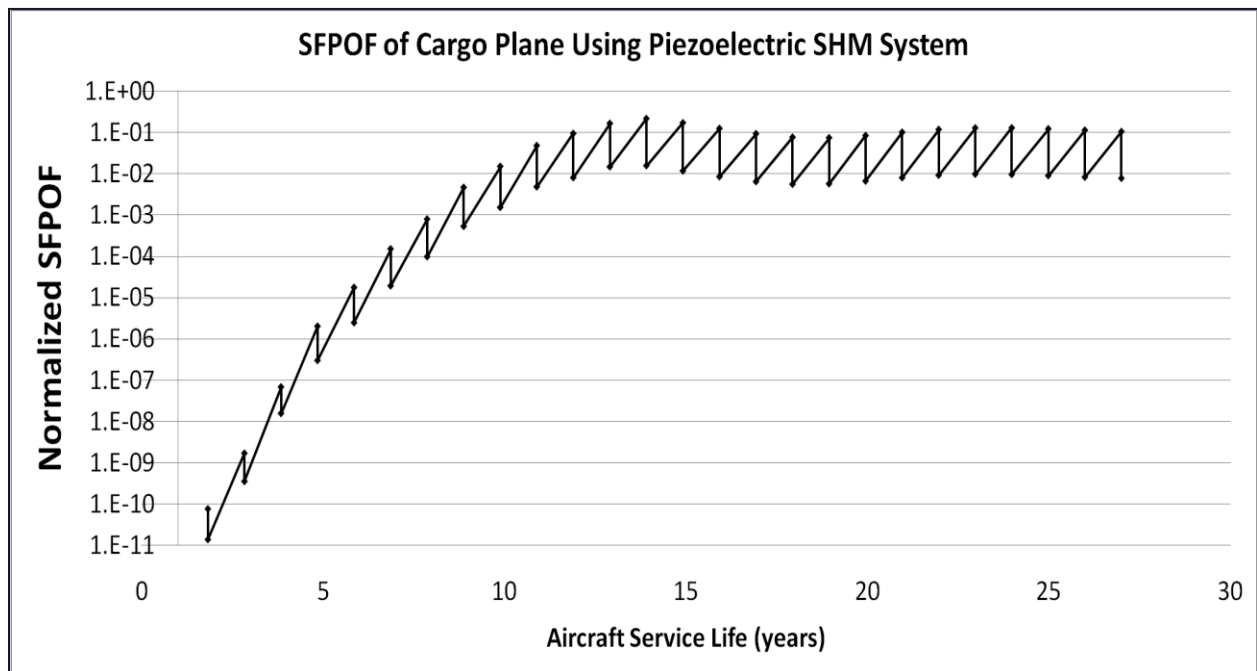


Figure 29. Piezoelectric SHM normalized single-flight probability of failure

Figure 30 plots the normalized SFPOF for the eddy-current SHM system for an inspection interval of 365 days. The plot shows the drastic effect that the POD of the inspection process can have on the associated risk. The eddy-current based SHM system that we based our POD estimates on had a much tighter POD. This leads to decreased risk because there is less probability of missing a crack that would lead to the stress of a flight exceeding the critical stress of the structure.

Both the piezoelectric SHM and the eddy-current SHM systems are viable solutions to implement with the USAF Structural Risk Methodology. This could be used to lower risk, while decreasing the amount of resources needed to maintain an air fleet. The amount of human resources needed to visually inspect an aircraft, especially a cargo lift aircraft, is

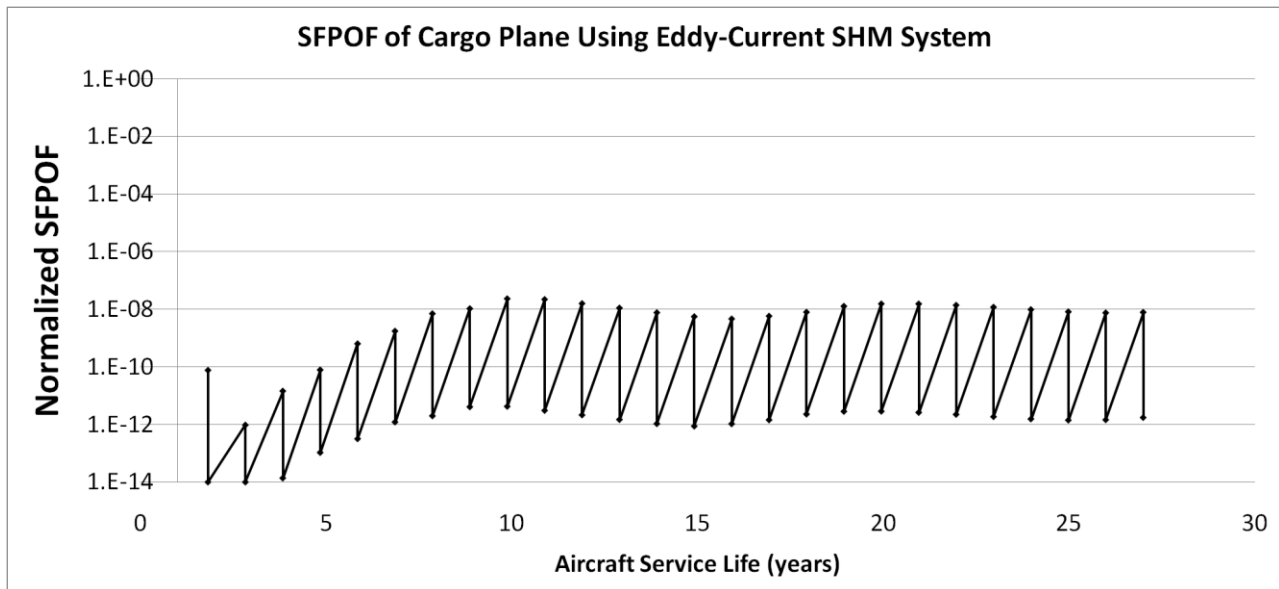


Figure 30. Normalized SFPOF for eddy-current SHM system

costly. In addition, the time needed to perform a complete magnetic-optic imaging (MOI) inspection is very costly and makes the airplane unavailable for an extended period of time. The ability to eliminate either process would result in substantial cost-savings. A piezoelectric SHM and eddy-current SHM system combined with the USAF Structural Risk Methodology could provide a safe method to eliminate both processes providing substantial savings in fleet management.

CHAPTER 5

CONCLUSION

In a world with limited resources and the threat of government budget cuts, it is critical to reduce the cost and resources needed to maintain aircraft. Currently, the Air Force uses periodic visual inspections and costly magneto-optic imaging (MOI) inspections to determine the health of cargo lift aircraft. However, this requires considerable manpower, cost, and subsequent aircraft downtime. In this thesis an alternative solution, a structural health monitoring (SHM) based risk analysis, was proposed that can reduce the resources needed, while keeping aircraft failure risk below acceptable levels. An SHM-based risk analysis uses a SHM system to perform periodic inspections of an aircraft structure's health. The results are then analyzed using the USAF Structural Risk Methodology and the subsequent probability of failure (POF), a measure of aircraft operational risk, is calculated.

A risk-based analysis using a SHM system is a viable solution to reduce maintenance costs, while keeping aircraft failure risk at acceptable levels. In this thesis, a risk analysis based on a piezoelectric SHM system and an eddy current SHM system was demonstrated. In order to perform the risk analysis, the POD for both SHM systems was estimated. For the piezoelectric SHM system, a laboratory experiment to estimate POD was performed on an aluminum test article. During the test, several simulated cracks were cut into the structure using a Dremel tool. A hit/miss analysis, as defined in MIL-HBK-1823A, was used to estimate the POD using results from the experiment. Due to limited resources, data from a published source was used to estimate the POD of the eddy current SHM system.

For the risk analysis, the USAF Structural Risk Methodology was used. The USAF Structural Risk Methodology was developed by the government to quantify the risk associated with operational aircraft and fulfill the United States Air Force (USAF) requirement for damage tolerant design. The USAF Structural Risk Methodology uses the Irwin Abrupt Fracture Criterion (J.P. Gallagher, 1984) to predict the

growth of a single crack on a critical aircraft structure. The result of USAF Structural Risk Methodology is a probabilistic distribution that predicts the risk of failure (P. Hovey A. B., 1998).

In order to demonstrate the viability of a SHM based risk analysis, an analysis was performed on both SHM systems. During the analysis, the POD for the SHM system was used as an input into the USAF Structural Risk Methodology. However, all other variables were left unchanged such as; mission loading parameters, geometric parameters, and material parameters. After the USAF structural risk analysis was performed the results were compared.

From the results, it is evident that a SHM based risk analysis is a feasible solution. Both systems were able to keep risks at or below acceptable levels, while increasing the time between inspections. In addition, both systems were able to eliminate the need for periodic visual inspections. More surprisingly, both systems were also able to eliminate the need for MOI inspections. However it should be noted that due to resource limitations, the POD for each system was estimated and the associated risk is highly dependent on the POD of the detection system. This is evident when comparing the risk profiles associated with the piezoelectric system and the eddy current system. For the piezoelectric system, laboratory experiments were used to estimate POD and the estimate was based on a conservative viewpoint. However, the eddy current system's POD was estimated using a source's data. Comparing the two PODs, the eddy current system has a much higher probability of detecting a crack of size, a , than the piezoelectric SHM system. The difference in POD caused drastic differences in the calculated risk. The eddy current system had substantially lower risk than the piezoelectric system, assuming identical inspection schedules. This is a result of the fact that POD is a measure of the probability of the inspection system detecting a crack of a specific size. Thus, a higher POD implies there is a smaller probability of not detecting a crack large enough to weaken the structure to a point that the loads experienced during operation exceed the critical load. Subsequently, a lower POD implies that there is a higher probability of a crack not being detected which would lead to higher risk. Thus, the POD of the inspection system should be fully characterized before integrating risk analysis with a SHM system.

Looking back, there are several opportunities to improve the system discussed in this paper. One area that would provide lower risk and much lower maintenance costs would be to optimize the maintenance and inspection process. By developing realistic cost functions for the inspection and maintenance program and defining the maximum acceptable level of risk, the optimal lowest cost solution could be determined. However, due to the length of time, the upfront investment costs and the subsequent maintenance costs for all inspection programs should be modified to take into account inflation and other capital investment costs. An optimal solution would provide substantial savings to the maintenance of the aircraft fleet while providing an acceptable level of risk. Another opportunity would be to integrate both the SHM system and the Structural Risk Methodology on the airframe and automate the inspection process completely. The current system requires a maintenance technician to provide power for the SHM system to perform the inspection. After the SHM system has completed the inspection, the resulting data is captured and then analyzed later. If both the SHM system and the USAF Structural Risk Analysis Software were integrated into the plane such that they had power and their own hardware the inspection process could be reduced to a maintenance technician grabbing the data after each flight. This would provide the capability to minimize the risk, while still providing a substantial reduction in regularly occurring maintenance costs. However, the upfront costs of integrating such a system would be fairly large and should be taken into consideration.

During this work, there was one other area that I see opportunities for additional work. There is a lack of quantification in the reliability of SHM systems. I feel there are several opportunities for improvements, particularly in the area of an integrated SHM system's POD. Currently, there doesn't seem to be a standard process for estimating the probability of detection of an integrated SHM system without extensive laboratory testing. In addition, the accuracy of this method is highly dependent on the test setup and the accuracy of a large set of measurements, leaving room for errors. However, there are several inherent difficulties about developing a method for estimating the POD of a complex integrated SHM system. First, the POD of most SHM systems is highly dependent on geometry and material properties. Second, there are several types of SHM sensors that measure unique values and are

affected differently by environmental effects. Third, since a complex SHM system is a network of many individual sensors, a complex SHM system could itself be composed of many different types of sensors. By adapting some of the techniques used to calculate PODs for individual sensors, I see an opening to create a standardized method of estimating the POD of a complex SHM system, even if several different types of SHM sensors are used together. Effectively, a POD matrix could be created that corresponded to locations on the structure for different crack sizes and then the resulting POD would be calculated from the POD matrix.

In conclusion, a USAF Structural Risk Analysis using a SHM system is a promising solution to decrease maintenance cost and minimize the risk of aircraft failure. Since the POD of the inspection system has a drastic effect on the probability of failure, a capable SHM system with an appropriate POD could eliminate the need for all other inspections saving money, time, and resources.

REFERENCES

- A. Coppe, R. H. (2008). A Statistical Model For Estimating Probability Of Crack Detection. IEEE.
- A.F. Grandt, J. (2004). Fundamentals of structural integrity: damage tolerant design and nondestructive evaluation. John Wiley & Sons, Inc.
- Achenback, J. D. (2009). From NDE To A Q To SHM And Beyond. Review Of Quantitative Nondestructive Evaluation , 28, 3-15.
- Berens, A. (1996). Applications Of Risk Analysis To Aging Military Aircraft. 41, 99-107.
- Department of Defense. (2009). Nondestructive Evaluation System Reliability Assessment. United States of America.
- E. Larson, B. P. (2000). A Subspace-Based Approach To Structural Health Monitoring. Digital Avionics Systems Conferences. 2, pp. 6C5/1 - 6C5/8 . IEEE.
- Gumbel, E. (1961). Bivariate Logistic Distributions. 56, 335-349.
- Gumbel, E. J. (1960). Multivariate External Distributions. 37, 471-475.
- J.P. Gallagher, F. G. (1984). USAF Damage Tolerant Design Handbook: guidelines for the analysis and design of damage tolerant aircraft structures. AFWAL-TR-82-3073.
- Leon-Garcia, A. (2008). Probability, Statistics, And Random Processes For Electrical Engineering (3 ed.). Pearson Prentice Hall.
- Mukkamala, R. (2000). Distributed Scalable Architectures For Health Monitoring Of Aerospace Structures. Digital Avionics Systems Conferences. 2, pp. 6C4/1 - 6C4/8. IEEE.

N. Goldfine, D. S. (2002). Surface Mounted And Scanning Periodic Field Eddy-Current Sensors For Structural Health Monitoring. Aerospace Conference Proceedings (pp. 6-3141- 6-3152). IEEE.

P. Hovey, A. B. (1998). Update Of The Probability Of Fracture (PROF) Computer Program For Aging Aircraft Risk Analysis. Air Force Material Command.

P. Hovey, J. G. (1983). Estimating The Statistical Properties Of Crack Growth For Small Cracks. 18, 285-294.

Peil, U. (2003). Life-Cycle Prolongation Of Civil Engineering Structures Via Monitoring. Structural Health Monitoring , 64-79.

R. Grimberg, L. U. (2005). 2D Eddy Current Sensor Array. NDT&E International , 39, 264-271.

R. Guratzsch, S. M. (2010). Structural Health Monitoring Sensor Placement Optimization Under Uncertainty. AIAA Journal , 48 (7), 1281-1289.

R.P. Reed, J. S. (n.d.). The economic effects of fracture in the United States.

Ross, S. (2004). Introduction To Probability And Statistics For Engineers And Scientist (3 ed.). Elsevier.

S. Beard, C. L. (2007). Design Of A Robust SHM System For Composite Structures. Industrial and Commercial Applications of Smart Structures Technologies , 6527, 1-9.

S. Bearda, A. K. (2005). Practical Issues In Real-World Implementation Of Structural Health Monitoring Systems. Smart Structures and Materials 2005: Industrial and Commercial Applications of Smart Technologies , 5762, 196-203.

S. Bo-Lin, S. B.-F. (2008). New Sensor Technologies In Aircraft Structural Health Monitoring. Conditional Monitoring And Diagnosis. Beijing, China.

Shantz, C. (2010). Uncertainty Quantification In Crack Growth Modeling Under Multi-Axial Variable Amplitude Loading. Vanderbilt University.

Sindel, R. (1998). Zur Untersuchung Von Systemen Von Ermüdungsrissen Bei Der Inspektionsplanung. Technological University, Munich, Germany.

V. Giurgiutiu, A. C. (2005). Embedded Non-Destructive Evaluation For Structural Health Monitoring, Damage Detection, And Failure Prevention. The Shock and Vibration Digest , 37 (2), 83-105.

W. Hines, D. M. (2003). Probability And Statistics In Engineering (4 ed.). John Wiley And Sons.

Weisstein, E. (n.d.). Gumbel Distribution from Wolfram MathWorld. (Wolfram MathWorld) Retrieved from MathWorld: <http://mathworld.wolfram.com/GumbelDistribution.html>

Y. Lu, J. M. (2009). Feature Extraction and Sensor Fusion for Ultrasonic Structural Health Monitoring Under Changing Conditions. Sensors , 9 (11), 1462-1471.

BIOGRAPHICAL INFORMATION

Jeff Tippey has a B.S. in Electrical Engineering from TCU and is finishing his M.S. of Electrical Engineering from University of Texas at Arlington. As an undergraduate, Jeff worked as a research assistant to Ed Kolesar primarily working on microelectromechanical systems (MEMS) design and modeling. Since graduating, Jeff worked at the Automation & Robotics Research Institute where he worked on MEMS actuator and sensor design. Currently, Jeff Tippey works at Lockheed Martin as a systems engineer.